On the Mesoscale Variability of Meteorological Fields – the Example of Southern Bavaria

H. Volkert

DFVLR, Institut für Physik der Atmosphäre, D-8031 Weßling

(Manuscript received 12.03.1985, in revised form 01.07.1985)

Abstract:

Detailed analyses of variance are carried out to obtain quantitative measures for the space and time dependence of anomaly patterns for single meteorological elements or several in combination. This pilot study uses Southern Bavaria (55 stations) and the years 1974 through 1977 as the test region and test period, respectively.

All analysed elements (pressure, temperature, relative humidity, cloud cover, daily sunshine duration and daily sum of precipation) exhibit a spatially independent proportion of variance on a scale larger than the test region, followed by a mesoscale north-south contrast. Characteristic time scales for the deviations from the mean annual fluctuation are of the order of a few days. Spatially larger structures posses longer time scales than the mesoscale ones.

Zusammenfassung: Zur mesoskaligen Variabilität meteorologischer Felder – das Beispiel Südbayern

Umfassende Varianzanalysen werden durchgeführt, um Maßzahlen zum räumlichen und zeitlichen Verhalten der Schwankungsstrukturen einzelner meteorologischer Elemente – oder mehrerer in Kombination – zu erhalten. Die vorliegende Pilotstudie verwendet Südbayern (55 Stationen) und die Jahre 1974 bis 1977 als Testgebiet und -zeitraum.

Alle analysierten Elemente (Druck, Temperatur, relative Feuchte, Bedeckungsgrad, tägliche Sonnenscheindauer und tägliche Niederschlagssumme) enthalten einen großräumigen (relativ zum Untersuchungsgebiet), ortsunabhängigen Varianzanteil als wichtigste Schwankungsstruktur, gefolgt von einem mesoskaligen Nord-Süd Gegensatz. Charakteristische Zeitskalen für die Abweichungen vom Jahresgang liegen im Bereich weniger Tage, wobei großräumige Strukturen längere Zeitskalen besitzen als mesoskalige.

Résumé: Sur la variabilité des champs météorologiques de mésoéchelle – L' exemple de la Bavière méridionale

On effectue une analyse détaillée de variance afin d'obtenir des évaluations quantitatives de la dépendance spatio-temporelle des anomalies d'éléments météorologiques particuliers ou de certaines de leurs combinaisons. Cette étude pilote concerne la Bavière méridionale (55 stations) et porte sur la période 1974 1977. Tous les éléments analysés (pression, température, humidité relative, nébulosité, durée de l' ensoleillement journalier et somme quotidienne des précipitations) présentent une composante de la variance indépendante de la position et d'échelle plus grande que la région testée, suivie d'un contraste nord-sud de mésoéchelle. Les temps caractéristiques des écarts à la moyenne annuelle des fluctuations sont de l'ordre de quelques jours. Les structures spatialement les plus étendues possèdent des échelles de temps supérieures à celles de la mésoéchelle.

1 Introduction

As one of several networks the German Weather Service (Deutscher Wetterdienst) maintains second-order climatological stations (Klimahauptstationen) where mainly honorary observers collect data on the same routine first introduced 200 years ago. The three daily observation times (7 a.m., 2 p.m., 9 p.m.) are sometimes called „Mannheimer Stunden" as the first meteorological networks was organized by the "societas meteorological palatina" (1780–1995), which had its centre at the Palatine

0005-8173/85/04 0498–19 $ 03.00/0

court in Mannheim (see CAPPEL, 1980). The main advantage of these data lies in the better spatial resolution relative to synoptic data and in the availability of longer records compared with special field experiments (e.g. MESOKLIP or MERKUR, carried through in the upper Rhine valley 1979 and in the Inn valley 1982, respectively).

The present study aims at exploiting this advantage, checking the data quality and covering the gap between detailed single station statistics (more "classical" studies e.g. by ATTMANNSPACHER, 1981; CAPPEL and KALB, 1976; SCHÄFER, 1982; research using advanced statistical techniques e.g. by FRAEDRICH and MÜLLER, 1983) and mere mean value maps of climatological fields (e.g. SCHIRMER and VENTSCHMIDT, 1979). So far, only a few papers deal with aspects of climatological anomaly patterns or of spatial correlations obtained from Central European data (e.g FLIRI, 1967; SCHÖNWIESE, 1979; HÜSTER, 1980), although the relevance of second moments for a statistical descriptions of the climate in a specific region is obvious (see e.g. CEHAK, 1982, p. 229; MASON, 1979, p. 210). This article should be considered as pilot study, which combines several techniques for the analysis and interpretation of both the space and time variability of meteorological fields. These techniques employ empirical orthogonal functions (EOFs), a frequency analysis of the coefficients that modulate the different EOFs and tests for the statistical significance of the results. In such a way one is able of obtain quantitative measures for the space and time dependence of anomaly patterns for single climatic elements or several in combination.

Southern Bavaria is chosen as a test region for various reasons. The vicinity of the Alps creates significant anomaly patterns with a typical lenth scale of 100 km or less (this is the meso-β scale in the nomenclature of ORLANSKI, 1975). The network of stations seemed appropriate in view of their density, even distribution and limited number (a test application should not require maximum resources). Also the advent of a numerical meso-scale model for the Alpine region and its surroundings motivated a data analysis in this area. The test period of the years 1974 through 1977 yields meaningful results, although future applications should use longer periods.

The body of this paper is divided into four sections. First in Section 2 the methododology is outlined and some notation introduced. A description of the data sets and the necessary preprocessing follow in Section 3. The various results obtained constitute the main part (Section 4), while Section 5 attempts to draw conclusions for further applications.

2 Methods and Notation

In this section the methodology and some notations for the present discussion are introduced. A somewhat broader overview is given by VOLKERT (1983).

We start from the covariance matrix **C** of a meteorological field **F** that is observed K times at p locations. In the following bold capital letters denote matrices; bold lower case letters stand for column vectors; the prime (′) indicates the transpose of a matrix or vector and · denotes matrix multiplication. **C** is of dimension p and its p^2 elements contain for every location the time averaged relation to the other p-1 stations (covariances) and to itself (autocovariance of simply variance):

$$\mathbf{C} = (c_{ij}) = (< f_i f_j >) = < \mathbf{f} \cdot \mathbf{f}' > \qquad i, j = 1, .., p; \text{ where} \qquad (1)$$

$$< f_i > = \frac{1}{K} \sum_{k=1}^{K} f_{ik} = 0 \qquad i = 1, .., p \qquad (2)$$

$$< f_i f_j > = \frac{1}{K-1} \sum_{k=1}^{K} (f_{ik} f_{jk}) \qquad i, j = 1, .., p \qquad (3)$$

f_{ik} denotes the anomaly of **F** at station i relative to the time average (or to fluctuations of low frequency, say the annual variation); the data vector $\mathbf{f}_k$ contains all p anomalies at time k; the brackets $< >$ stand for time averaging operators that produce unbiased estimates for both means values (Equation 2) and variances (Equation 3).

The eigenvectors of covariance matrices constructed from geophysical data are often called empirical orthogonal functions (EOF) following LORENZ (1959). In comparison to mathematical functions (e.g. trigonometric or Legendre polynomials) they are calculated from observed data and thus are defined only at the discrete locations where the data are available. As the covariance matrix is real, symmetric and positive definite they constitute an orthogonal system with non negative eigenvalues.

We summarize the properties of the EOFs v_i and the corresponding eigenvalues λ_i, which are assumed to be arranged in descending order ($\lambda_i \geqslant \lambda_{i+1}$; i = 1, .., p-1):

$$\mathbf{C} \cdot \mathbf{v}_i = \lambda_i \mathbf{v}_i \quad \text{with} \quad \mathbf{v}_i' \cdot \mathbf{v}_j = \sum_{n=1}^{p} v_{in} v_{jn} = \delta_{ij} \qquad i, j = 1, .., p$$

$$\mathrm{Spur}(\mathbf{C}) = \sum_{i=1}^{p} \lambda_i = \Lambda$$

As the diagonal elements of **C** contain the variances at the single stations, Λ is a measure for the total variance of the element in view (which, of course, depends on the number of stations p). The relative magnitude of each eigenvector (λ_i/Λ) characterizes the proportion of variance represented by $\mathbf{v}_i$. This is further clarified by the expansion of the data vectors $\mathbf{f}_k$ as a linear combination of the eigenvectors

$$\mathbf{f}_k = \sum_{i=1}^{p} a_{ik} \sqrt{\lambda_i}\, \mathbf{v}_i \qquad\qquad k = 1, .., K$$

where $\sqrt{\lambda_i}$ carries the absolute value and the physical dimension of each term, while both the eigenvectors $\mathbf{v}_i$ and the amplitude coefficients a_{ik} are dimensionless and orthonormal in space and time, respectively.

Of most practical importance is the "optimal approximation property" of EOFs. For any incomplete summation with $q < p$, Equation 6 yields that approximation $\mathbf{e}_k^q$ to the data vector $\mathbf{f}_k$, which produces the minimum mean square error E^q (see DAVIS 1976, p. 265):

$$E^q = < (\mathbf{f} - \mathbf{e}^q)' \cdot (\mathbf{f} - \mathbf{e}^q) > = \Lambda - \sum_{i=1}^{q} \lambda_i \qquad q = 1, .., p-1$$

Thus, after setting up the covariance matrix and inverting it by standard library routines we check whether a significant proportion (80%) of the overall variance can be explained by a few ($q/p < 0.1$) EOFs. Their spatial structures identify regions within which the observed fluctuations are either positively or negatively correlated, or not at all. Before a physical interpretation is attempted, the significance of the results (against ones obtained from random data) has to be tested.

Only recently PREISENDORFER et al. (1981) introduced a sound mathematical foundation for the problem of testing the statistical significance of EOFs (at least in the geophysical context). Here we adopt their selection rule N which we summarize briefly (see also OVERLAND and PREISENDORFER, 1982).

First we state as null hypothesis that the data set, from which the relative eigenvalues $T_i = \lambda_i/\Lambda$ are calculated, is randomly drawn form a population of uncorrelated Gaussian variables. Then p independent sequences of length K and with zero mean and unit variance are evaluated by a random number generator. From these random data we compute the covariance matrix and their relative eigenvalues, repeat this random experiment r times (e.g. r = 100) and rearrange the relative eigenvalues U_i^s (s = 1, .. r) in ascending order for each EOF number i. After choosing a significance level α (e.g. $\alpha = 0.05$) the null hypothesis can be rejected for all EOFs with $T_i > U_i^t$ [$t = 1 - \alpha)r$] and an attempt to interpret these non-random EOFs physically seems to be reasonable. The key point of this significance test on a Monte Carlo basis lies in the adoption of the number of stations p and the number of observations K from the meteorological data set. In Table 1 the dependence of the threshold values U_i^{95} on p and K is listed for r = 100, $\alpha = 0.05$. The covariance matrix obtained from random data degenerates to the unity matrix with p identical relative eigenvalues $U_i = 1/p$ (i = 1, .., p) only for infinitely long time series ($K \rightarrow \infty$).

The significant non-random eigenvectors determine those spatial structures of the anomaly patterns that are most dominant during the whole observation period. This average feature results from the definition of the covariance matrix as a time averaged quantity (see Equation 3). Therefore it is also necessary to assess the dependency of EOFs on the sampling period.

The temporal behaviour of a single EOF $\mathbf{v}_i$ can be studied by inspection of the time series of its amplitude coefficient a_{ik} (k = 1, ..,K). Via a frequency analysis we determine a typical time scale τ as a quantitative measure for each amplitude coefficient. A general description of this procedure is given in standard text-books (e.g. JENKINS and WATTS, 1968), while a precise outline for climatological applications can be found in MITCHELL (1966). Here we summarize the main points.

■ **Table 1** Significance levels U_i^{95} for relative eigenvalues T_i dependending on the number of stations (p), the eigenvalue order (i) and the length of the timeseries (K). Part A from OVERLAND and PREISENDORFER (1982); part B calculated for this study.

p	i	K: 20	60	100	200	1000	1460	∞
9	1	.298	.248	.183	.159	.131	---	.111
	2	.220	.173	.157	.143	.124	---	.111
	3	.179	.150	.141	.132	.121	---	.111
15	1	---	---	---	---	---	.081	.067
	2	---	---	---	---	---	.079	.067
	3	---	---	---	---	---	.076	.067
36	1	.150	.087	.069	.056	.039	---	.028
	2	.127	.076	.065	.051	.038	---	.028
	3	.109	.070	.059	.049	.037	---	.028
51	1	---	---	---	---	---	.028	.020
	2	---	---	---	---	---	.027	.020
	3	---	---	---	---	---	.026	.020
64	1	.120	.065	.050	.037	.025	---	.016
	2	.107	.059	.046	.036	.024	---	.016
	3	.095	.054	.043	.034	.023	---	.016
100	1	.105	.053	.040	.029	.017	---	.010
	2	.093	.048	.037	.028	.017	---	.010
	3	.086	.046	.036	.027	.017	---	.010
153	1	---	---	---	---	---	.012	.007
	2	---	---	---	---	---	.011	.007
	3	---	---	---	---	---	.011	.007

Part A (columns K = 20 to 1000) — Part B (columns K = 1460 and ∞)

The discrete spectrum of the time series is calculated as the Fourier transform of the time lagged autocovariance function. Thus, one obtains estimates for the contribution C(f) of the frequency band $[f-\Delta f/2, f+\Delta f/2]$ to the overall variance, where the frequency f is bounded by the Nyquist frequency $f_N = 1/(2\Delta t)$ [Δt: sampling interval] and the spectral resolution Δf depends on the maximum time lag $u = l_{max}\,\Delta t$ as $\Delta f = f_N/l_{max} = 1/(2u)$. This sample spectrum has to be compared with the spectrum of a statistical model process.

In our case the discrete, linear, first order Markov or red noise process seems most appropriate, as it takes into account the persistence that is generally evident in climatological time series besides a random component Z_k. Formally this process reads

$$X_k = R\,X_{k-1} + Z_k \quad \text{with} \quad 0 \leqslant R < 1; \quad \langle Z_k \rangle = 0; \quad \langle Z_k\,Z_k \rangle = \sigma_Z^2 \tag{8}$$

The formal parameter R is equivalent to the (lag-one) autocorrelation function of the process and thus a direct measure for its persistence. The corresponding spectrum (see e.g. JENKINS and WATTS, 1968, p. 228)

$$\Gamma(f) = \frac{(1-R^2)\,\sigma_Z^2/f_N}{1 + R^2 - 2R\cos(\pi f/f_N)} \qquad 0 \leqslant f \leqslant f_N \tag{9}$$

is more pronounced at low frequencies as R approaches unity, while it degenerates to the white noise spectrum $\Gamma(f) = \sigma_Z^2/f_N$ for $R = 0$.

For a particular series of amplitude coefficients R is evaluated by fitting the theoretical spectrum $\Gamma(f, R)$ to the sample spectrum C(f) according to the condition

$$\sum_{i=0}^{l_{max}} \{\Gamma(f_i, R) - C(f_i)\}^2 = \text{minimum} \qquad f_i = i\,\Delta f. \tag{10}$$

Thus, we assume as a working hypothesis for the timescales under consideration that all data can be seen as realisations of first order Markov processes. As a measure for the persistence we then use a characteristic timescale $\tau = -\Delta t/\ln(R)$ during which period the autocovariance function reduces to 1/e of its original value.

To assess the quality of our fit we use the fact that for every frequency, the ratio of sample to theoretical spectral estimate follows a $\chi^2(n)/n$ – distribution with $n = 2K/l_{max} - 1/2$ degrees of freedom (MITCHELL 1966, p. 40). So we are able to establish, say, the 95 % confidence interval of the theoretical spectrum and check whether the sample spectrum exhibits significant peaks or gaps. If this is not the case, we conclude that the times series under consideration shows only random variations besides a persistence with characteristic timescale τ, but no significant periodicities.

Finally, we note the inverse dependence of the confidence interval and the spectral resulution on the maximum time lag $u = l_{max}\Delta t$. Small (large) l_{max} leads to a coarse (fine) resolution, but to a sharp (meaningless) confidence interval. For our applications $l_{max} = K/8$ has proven to be a reasonable compromise.

3 Data

Data collected at the climatological stations (given in Figure 1 and Table 2) during the period 1/1/1974 through 31/12/1984 constitute the basis for this study. Temperature, relative humidity and cloud cover are recorded three times per day (7 a.m., 2 p.m., 9 p.m.) at all 55 stations, as well as the daily sum of precipitation (from 7 a.m. to 7 a.m. of the following day); the daily sunshine duration is measured only at 37 stations (compare Figure 4d) and the pressure at 12 synoptic stations (compare Figure 4f).

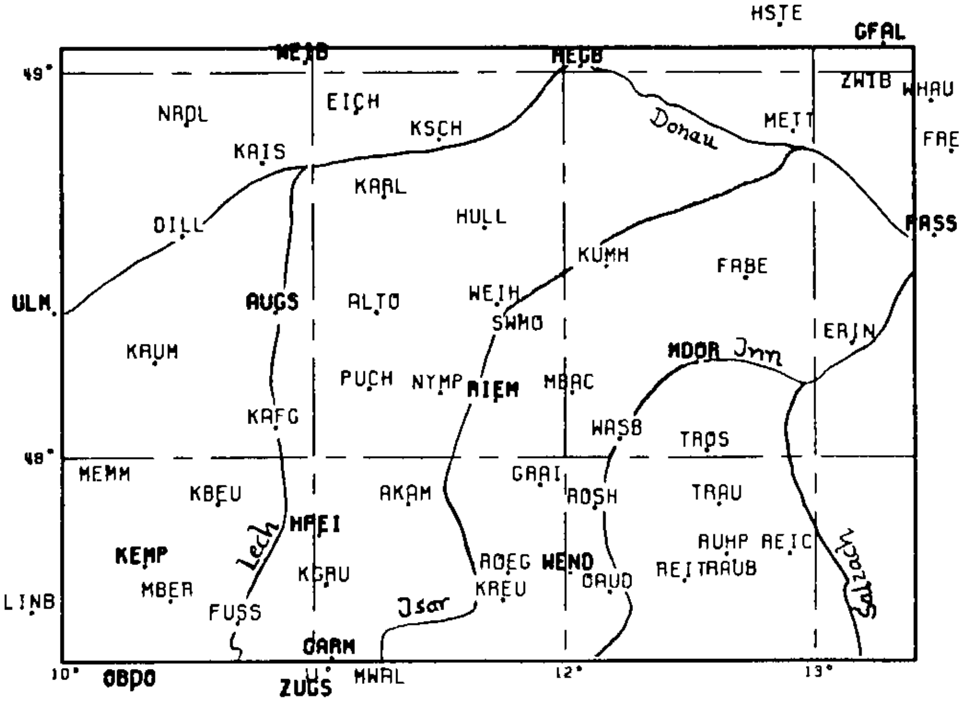

Figure 1
Map of Southern Bavaria with second order climatological stations in operation from 1974 through 1977 and major rivers. Subsample of synoptic stations in bold letters. See Table 1 for the abbreviation codes.

Table 2 Climatological stations in Southern Bavaria where complete datasets are available for the period 1974–77 (for the geographical distribution see Figure 1)

Station	Code	Station	Code	Station	Code
Nördlingen	NRDL	Schwaigermoos	SWMO	Attenkam	AKAM
Kaisheim-Neuhof	KAIS	Kumhausen	KUMH	Rottach-Egern	ROEG
Weißenburg	WEIB	Falkenberg	FABE	Wendelstein	WEND
Eichstätt	EICH	Ering	ERIN	Rosenheim	ROSH
Kösching	KSCH	Passau	PASS	Traunstein-Kotzing	TRAU
Regenburg	REGB	Memmingen	MEMM	Ruhpolding	RUHP
Höllenstein	HSTE	Krumbach	KRUM	Rauschberg	RAUB
Metten	METT	Kaufering	KAFG	Bad Reichenhall	REIC
Zwieselberg	ZWIB	Puch	PUCH	Lindenberg	LINB
Gr. Falkenstein	GFAL	München-Nymphenburg	NYMP	Oberstdorf	OBDO
Waldhäuser	WHAU	München-Riem	RIEM	Mittelberg	MBER
Freyung	FREY	Großhöhenrain	GRAI	Füssen-Horn	FUSS
Ulm	ULM	Mittbach	MBAC	Zugspitze	ZUGS
Dillingen	DILL	Wasserburg	WASB	Bad Kohlgrub	KGRU
Augsburg	AUGS	Mühldorf	MDOR	Garmisch	GARM
Altomünster	ALTO	Trostberg	TROS	Mittenwald	MWAL
Karlshuld	KARL	Kempten	KEMP	Kreuth	KREU
Hüll	HULL	Kaufbeuren	KBEU	Oberaudorf	OAUD
Weihenstephan	WEIH	Hohenpeißenberg	HPEI	Reit im Winkel	REIT

For comparisons concerning the data quality the synoptic observations (00, 03, ..., 21 GMT) are available for the stations which are given bold letters in Figure 1. It must be noted that this data set is not complete as only the stations REGB, PASS AUGS, RIEM and ZUGS operate around the clock, while the remaining ones obtain only a mean observation rate of 77 % for the 1974/77 period due to breaks of varying length during the night hours.

As in any statistical study the representativeness of the chosen sample (the 1974/77 period in our case) should be assessed. In our case some independent material is available. A comparison of mean temperature and precipitation between the periods 1931/60 (SCHIRMER, 1969) and 1974/77 is possible for 23 stations; the latter period was slightly warmer everywhere (about 0.5 K) and a little more rainy at the majority of places (about 8 cm/a; see VOLKERT, 1983, pp. 32–33 for detailed figures). An internal investigation by the Wetteramt München allows a comparison of the annual sunshine duration for 15 stations and the periods 1951/60 versus 1974/77. It reveals a reduced insolation during the latter episode (about 50 h/a).

There is a paucity of values for observed variabilities in the literature. SCHÖNWIESE (1974, p. 136) gives temperature variances derived from monthly means for the period 1860/1960 at München and Hohenpeißenberg. Table 3 compares these values with our results. Although related to different mean values, the variances of both samples agree very well. At the elevated station (Hohenpeißenberg in 1000 m MSL) the mean temperature deviation is slightly smaller than over the plain (München, 500 m MSL).

In summary, it was found very difficult to assess the representativeness of the chosen period. SCHÖNWIESE (1979a, p. 9) illustrates well the general problem of defining an appropriate length of averaging periods in climatology by pointing out that the last official WMO period (1931/60) was for many places one of the few exceptionally warm ones within the last millenium. However, comparisons with the independent data available suggest that the sample under consideration might reveal statistical characteristics typical for Southern Bavaria. At the same time the need for variability studies of meteorological elements becomes evident.

Before performing an analysis of spatial variability structures with help of the EOF technique, the portions of the overall variance, which would obscure the results, have to be removed. In our case they consist of the inter-annual and annual variations and the fluctuations with the time of day.

Amplitude and phase of the annual variation and those with longer periods (i.e. T_1 = 4 a, T_2 = 2 a, T_3 = 1.33 a, T_4 = 1 a) are determined from the data by a Fourier analysis, separately for every station and every element. This procedure has the advantage that the low frequency variability is obtained objectively and that the remaining variance lies exactly in that portion of the spectrum which can be resolved by means of a frequency analysis.

Figure 2 gives the original noon temperature and the compound annual fluctuation at München-Riem during the entire four year period. The mean value of 11.7 °C is modulated by a pronounced annual wave with an amplitude of 9.5 K and its maximum on July 16 (day 197), whereas the small waves with longer periods and amplitudes of less than 0.5 K are responsible for the slightly different times (up to 6 days) at which the mean is passed in the different years. Only the remaining positive and negative deviations enter the EOF analysis.

Having recognized the dominance of the annual wave in the noon temperature, it is important to observe its spatial variability. The amplitude attains its maximum (10.6 K) at several stations in the Da-

■ Table 3 Mean (M), mean square (S^2) and root mean square (S) of temperature at München and Hohenpeißenberg for the periods 1860/1960 and 1974/77

Period	1860/1960			1974/77		
quantity	M	S^2	S	M	S^2	S
units	°C	K^2	K	°C	K^2	K
München	7.7	53.4	7.3	8.3	52.0	7.2
Hohenpeißenberg	6.2	42.1	6.5	6.7	48.6	7.0

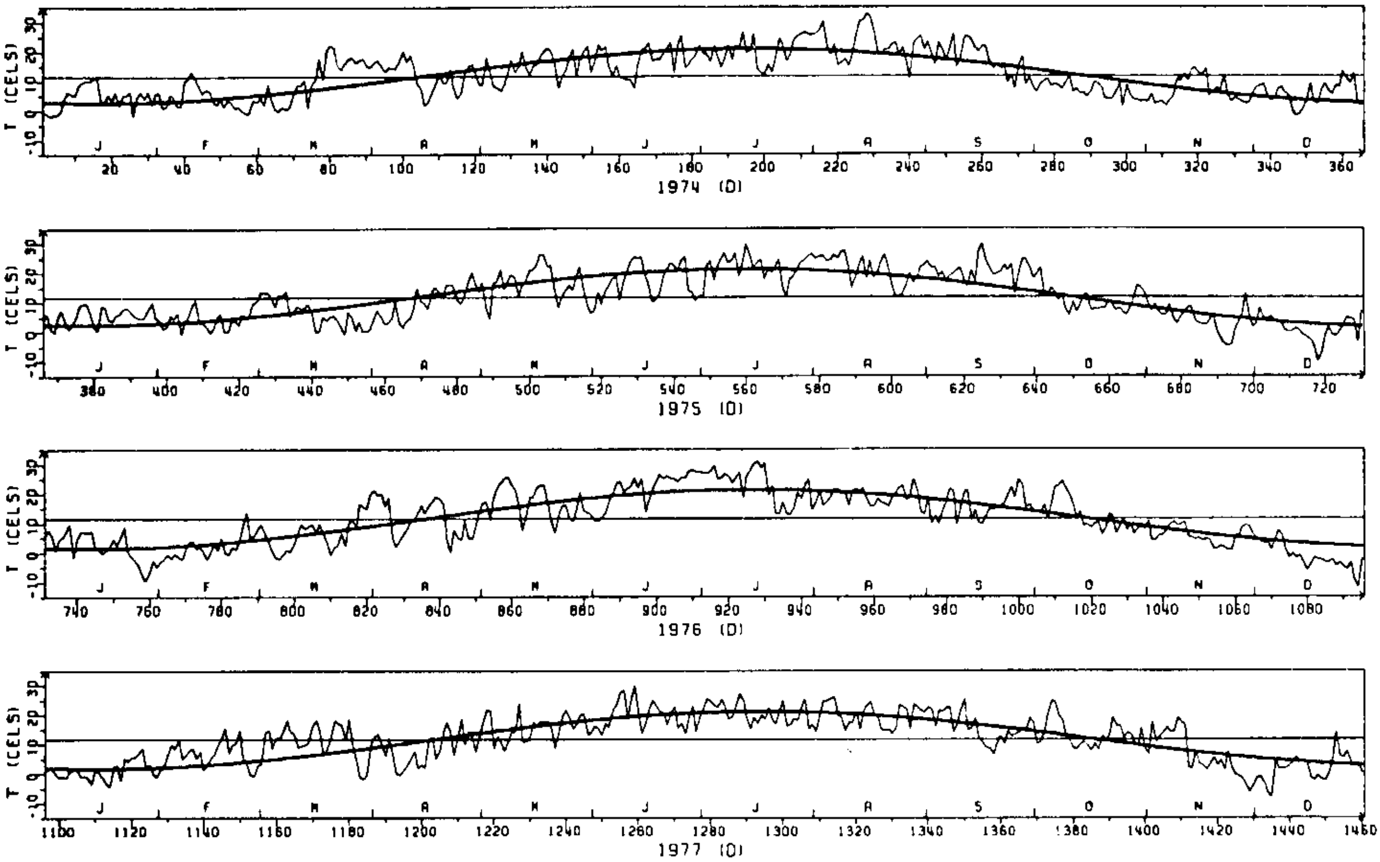

Figure 2

Noon temperature (14 hours local time) at München-Riem in 1974 through 1977 (thin line) with mean value (11.7 °C) and compound Fourier mode annual variation (thick line; see text for details).

nube plain, decreases towards the Alps and the Bayerischer Wald (to about 8.5 K) and attains its minimum at the mountain stations (RAUB: 7.6 K at 1640 m MSL; WEND: 7.0 K at 1830 m MSL; ZUGS: 6.7 K at 2960 m MSL). The phase exhibits a similar trend correlated with the station height. The extrema occur in the Danube plain five days before the reach the Alpine valleys, and there is a lag of another ten days before they reach the summits (for details see VOLKERT, 1983, pp. 64–65).

This example highlights the difficulties which can arise during the attempt to correlate observations from differently elevated stations. Although the removal of the annual fluctuations is station dependent and thus smooths respective differences in the raw data, the summit stations (GFAL, WEND, RAUB, ZUGS; all above 1500 m MSL) are not considered in most of the following analyses, as they hardly contain information for the planetary boundary layer.

The second source of variance, which is irrelevant for the present incestigation, lies in the diurnal variation. No special attention is necessary for the "integral elements" sunshine duration and precipitation and for the daily averaged, smooth and spatially poorly resolved pressure field. For the "momentary elements" temperature, humidity and cloud cover, however, independent analyses are carried out for every observation time (i.e. 7, 14, 21 hours). Thus, the variance portion between the different times of day is eliminated, which amounts to 10 %, 30 % and 1 % of the overall variance of the compound series for temperature, humidity and cloud cover, respectively.

Table 4 gives an overview of the analyses which are carried out. Elements and network sizes are as already mentioned. The third row contains the total variances (summed over all stations) of the raw data and its proportions which are caused by the compound, low frequency Fourier mode, annual fluctuactions. These fluctuations are nearly neglegible for pressure, humidity and precipitation, while

■ **Table 4** Global variability measures for the elements pressure (P), temperature (T), relative humidity (H), cloud cover (C), sunshine duration (S) and precipitation (R). Analysed are either daily means (M) or sums (Σ) or observations from specific times (7, 14, 21 hours) obtained from a varying number of stations (p). Absolute values are given for the total variance (TV) and the analysed variance (AV; AV = TV x (100-PAF)/100). PAF denotes the proportion of the compound annual fluctuation within TV, while λ_i/Λ (i=1, .., 5) stands for the proportion of AV expained by EOFi (*non-significant values in italics*). q_{sig} EOFs differ significantly from random data; together they explain the proportion $\Sigma\lambda/\Lambda$.

Element units	P hPa²	T K²			H 1			C 1			S h²	R mm²
Analysis	M	7	14	21	7	14	21	7	14	21	Σ	Σ
p	12	51	51	51	51	51	51	51	51	50	37	51
TV	629	2470	3640	2440	0.52	1.89	0.74	7.13	5.61	8.53	663	2310
PAF	6%	71%	65%	71%	11%	23%	20%	7%	3%	6%	21%	3%
AV (=Λ)	593	723	1240	713	0.46	1.42	0.59	6.63	5.36	8.02	518	2240
λ_1/Λ	98%	81%	89%	85%	46%	69%	54%	60%	64%	60%	78%	64%
λ_2/Λ	*1.0%*	6.1%	3.7%	3.9%	15%	9.0%	11%	7.9%	7.7%	6.9%	6.5%	6.8%
λ_3/Λ	*0.3%*	*2.6%*	*2.3%*	*2.0%*	7.2%	5.0%	5.5%	5.5%	4.7%	4.9%	4.8%	5.4%
λ_4/Λ	*0.1%*	*2.1%*	*1.0%*	*1.6%*	3.9%	3.0%	4.2%	3.5%	3.0%	2.8%	*2.0%*	3.2%
λ_5/Λ	*0.1%*	*1.0%*	*0.5%*	*0.8%*	*2.4%*	*1.4%*	*2.2%*	*1.8%*	*1.6%*	*1.6%*	*1.2%*	*2.0%*
q_{sig}	1	2	2	2	4	4	4	4	4	4	3	4
$\Sigma\lambda/\Lambda$	98%	87%	93%	89%	72%	86%	74%	77%	80%	74%	89%	80%

they contain one fifth of the sunshine and humidity total variances and even two thirds of the temperature variability. The spatial structure and relative importance of the EOF-patterns from the remaining variances (AV or Λ of Equation (5)) constitute the main topic of the next section.

4 Results

The full results which can be extracted from the available climatological data by the means discussed in Section 2 are documented in VOLKERT (1983). Here we concentrate on the main features, which comprise in sequence global measures, the spatial structures of single EOFs, frequency spectra and time scales, compound analyses of several elements, and the stability of EOFs.

The global measures of the analyses carried out are given in the fourth row of Table 4. The covariance matrices of all elements clearly possess dominant eigenvalues λ_1. The latter show a rank order from the "purely large scale" elements (relative to the area under consideration; pressure and temperature) to ones significantly influenced by meso scale structures (humidity, cloud cover, precipitation). Furthermore we observe a daily variation within the relative contricutions to the overall variance. At noon, λ_1 explains a greater portion of variance than in the morning or evening hours, when the connections within one element are more likely to be locally disturbed. This is particularly evident with humidity. The low value of λ_1 within the 7 hours analysis can be explained qualitatively as due to the humidity reduction in the morning that takes places either before of after the measurement at the various stations. From the noon analyses we conclude that all elements possess a maximum of four significantly non-random eigenvalues and their corresponding EOFs explain at least 80 % of the overall variances.

Figure 3 exemplifies the spatial structures of EOF1. Nearly all elements exhibit the same constant field as that of temperature (Figure 3a); only the pattern for the daily precipitation shows a slight north-south gradient. Although all EOFs are only discretely defined at the stations, the maps in Figures 3, 4, 5, 7 contain isolines to aid optical comparisons. For reference the values at stations are given in Figures

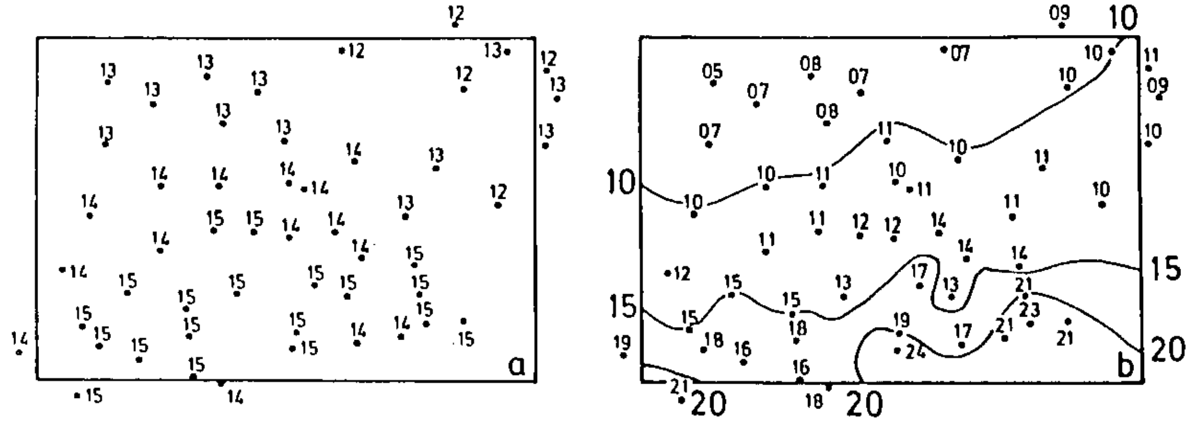

Figure 3
EOF1 for temperature (a; noon values) and precipitation (b; daily sums). All numbers are in hundredths of dimensionless units (compare Equation (4)).

3, 4a, 4f. All numbers are in hundredths of dimensionless units (compare Equation (4)). The fact that all components of EOF1 are positive is equivalent to the observation of only positive elements in the covariance matrices, while the constancy of EOF1 indicates that the time series at all stations exhibit similar variances. Thus, an equal deviation (either positive or negative) form the mean annual variation is the most characteristic climatic state for the entire region of Southern Bavaria, even if it is never realized on a single day. The gradient in EOF1 of the precipitation field agrees with the well known fact that rainfalls in the pre-Alpine region tend to be heavier than further to the north.

The most important modulation structures on top of the constant deviation described by EOF1 are visualized by EOF2 (Figure 4). A uniform north-south gradient (with a small inclination towards southwest) shows up as a main feature in the patterns for temperature, humidity, cloud cover and sunshine duration. The most pronounced contrasts exist between the Allgäu and the Danube region of Lower Bavaria, whereas the values in the Bayerischer Wald resemble those of the eastern parts of Upper Bavaria. EOF2 of the pressure has a similar structure (Figure 4f), although the low relative eigenvalue λ_2/Λ (compare Table 4) indicates that the pressure anomaly of Southern Bavaria is nearly uniform.

The second eigenvector of the precipitation covariance matrix is different (Figure 4e). It exhibits a west-east contrast, which is modified by the Alpine foothills. The strongest difference exists between Allgäu and Chiemgau. This structure may be explained with the synoptic experience of a pronounced time lag (> 1 day) in the conset times of heavy rainfalls between the western and eastern parts of the windward side of the Alps. As the opposite happens at the end of many precipitation periods, this delay is resolved by the analysis of daily sums of precipitation.

Figure 5 shows EOF3 of humidity as an example of the spatial structures of higher EOF modes. Both display a west-east contrast. In the first case Swabia is in opposition to the rest of the region, in the second case Upper Bavaria.

Figures 3 to 5 depict ten out of the 38 significantly non-random EOFs for which global figures are given in Table 4. In order to assess the similarity of the remaining EOFs with the depicted ones we use the scalar product as a concise measure. Here the scalar product between vectors v_1 and v_2 is defined to be equal to $|v_1' \cdot v_2'|$ (see Equation (4)); a scalar product value of 1 indicates equality of the unit vectors $\mathbf{v}_1$ and $\mathbf{v}_2$, a value of 0 shows their orthogonality; when EOF from different networks are compared, only the common stations are taken into account (adequately weighted). The upper part of Table 5 quantifies the already stated great similarity between the EOF1s and the EOF2s, respectively, of the six major analyses (P, T14, H14, C14, S, R) and shows the different structure apparent in the precipitation EOFs. For the analyses T14, H14, C14 and S this similarity extends to the third

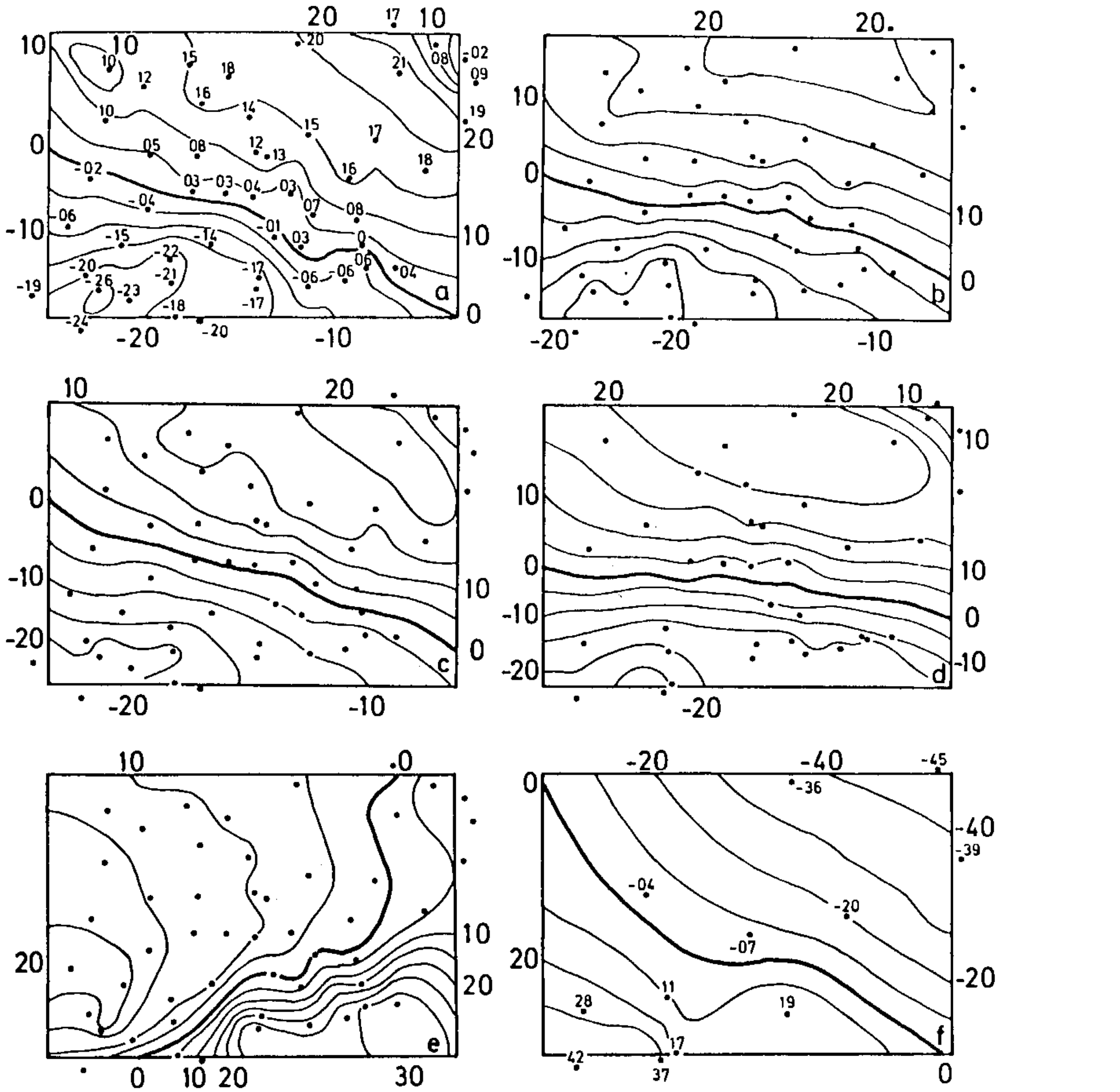

Figure 4

EOF2 for temperature (a), relative humidity (b), cloud cover (c), sunshine duration (d), precipitation (e) and pressure (f); (a) to (c) are calculated from noon values, (d) and (e) from daily sums and (f) from daily means; in (a) and (f) values (in hundredths) at stations are given to demonstrate the quality of the isoline analysis.

and fourth EOF mode. In the lower part of Table 5 the time of day is the varying parameter within analyses of temperatur, humidity and cloud cover, respectively. EOF1 is always of the constant field type. Within EOF2 discrepancies are discernible, mainly due to local disturbances in the morning and evening patterns; the latter two tend to be quite similar to each other for temperature and humidity.

The global measures obtained from analyses of data synoptic stations are given in Table 6. The raw data consist of averages over the well documented daytime period 06 to 18 hours for pressure, temperature relative humidity and cloud and of daily sums for sunshine duration and precipitation. Except for the reconstructed humidity (relative humidity is calculated from the measured air and dew point tempe-

■ **Table 5** Similarity of different EOFs measured by the scalar product. Upper part: EOF1 to EOF4 of different elements (see Table 4 for abbreviations). Lower part: EOF1 and EOF2 of the same element at different times of day. *Italics indicate analyses for which the appropriate EOF is depicted in Figures 3 to 5.*

Element	P	*T14*	H14	C14	S	R	T14	*H14*	C14	S
				EOF1					EOF3	
P		1.00	0.99	1.00	1.00	0.95				
T14	0.93		1.00	1.00	1.00	0.96	---	0.98	0.97	0.91
H14	0.92	0.96	---	1.00	0.99	0.96	0.94	---	0.94	0.92
C14	0.96	0.96	0.97		0.99	0.96	0.91	0.92	---	0.84
S	0.92	0.93	0.98	0.96		0.94	0.85	0.95	0.89	---
R	0.22	0.05	0.18	0.05	0.45	---				
			EOF2					EOF4		

	Temperature			Humidity			Cloud Cover		
Time	07	*14*	21	07	*14*	21	07	*14*	21
		EOF1			EOF1			EOF1	
07	---	1.00	1.00	---	0.94	0.96		1.00	0.98
14	0.84	---	1.00	0.77	---	0.98	0.95	---	0.98
21	0.95	0.91	---	0.93	0.89	---	0.91	0.91	---
	EOF2			EOF2			EOF2		

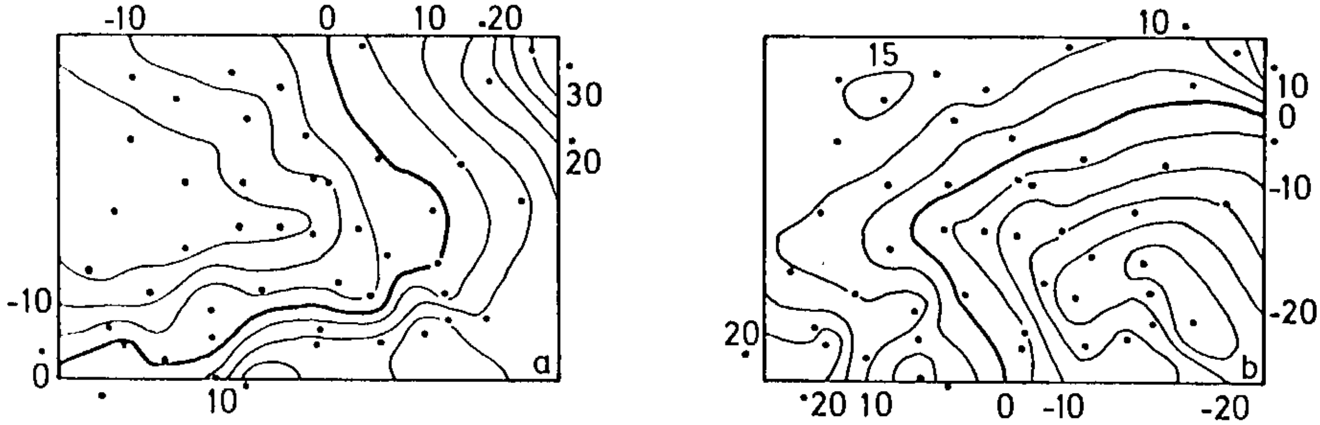

● **Figure 5** Relative humidity: EOF3 (a) and EOF4 (b). Labels in hundredths of dimensionless units.

ratures using Magnus' formula), the proportion of the total variance due to the compound annual fluctuation coincides with the values obtained from climate station data (compare Table 4). The significantly non-random relative eigenvalues (at most two due to the low number of stations; compare Table 1) are close to their climate station counterparts. EOF1 is again a constant field (except for precipitation), while a clear north-sourth contrast in EOF2 is found only for cloud cover and sunshine; this is quantified by the scalar product in the last row of Table 6.

For two reasons the comparison between synoptic and climate station data is far from perfect. First, the low number of synoptic stations available makes it necessary to include the mountain stations GFAL, WEND and ZUGS (see Table 2), if a minimum of spatial resolution is desired. Then the use of a daytime mean is only a compromise to avoid too large a variety of synoptic data analyses. However, since the global measures agree so well, the conclusion seems to be well justified that the quality of the climate station data is sufficient for the comprehensive analyses of variance carried out here. Thus, in our context, a better spatial resolution makes the climate stations superior to the synoptic ones.

■ **Table 6** Global variability measures for analyses based on data from synoptic stations (see Table 4 for abbrevations). Analysis type M denotes mean values from the well documented period 06 to 18 hours. The last row contains scalar products with the EOFs from climate station data.

Element units	P hPa^2	T K^2	H 1	C 1	S h^2	R mm^2
Analysis p	M 15	M 15	M 15	M 15	Σ 15	Σ 15
TV	816	851	0.37	1.31	224	623
PAF	94%	30%	72%	93%	78%	98%
AV (= Λ)	771	253	0.27	1.23	287	608
λ_1/Λ	98.4%	85.0%	60.4%	73.8%	74.9%	62.2%
λ_1/Λ	*0.9%*	*7.4%*	15.8%	9.1%	8.5%	8.3%
λ_3/Λ	*0.3%*	*2.7%*	*7.4%*	*4.8%*	*4.9%*	*6.4%*
q_{sig}	1	1	2	2	2	2
$\Sigma\lambda/\Lambda$	98.4%	85.0%	76.2%	82.2%	83.4%	70.5%
EOF1 · EOF1	1.00	1.00	0.99	1.00	1.00	1.00
EOF2 · EOF2	0.80	0.52	0.49	0.99	0.99	0.80

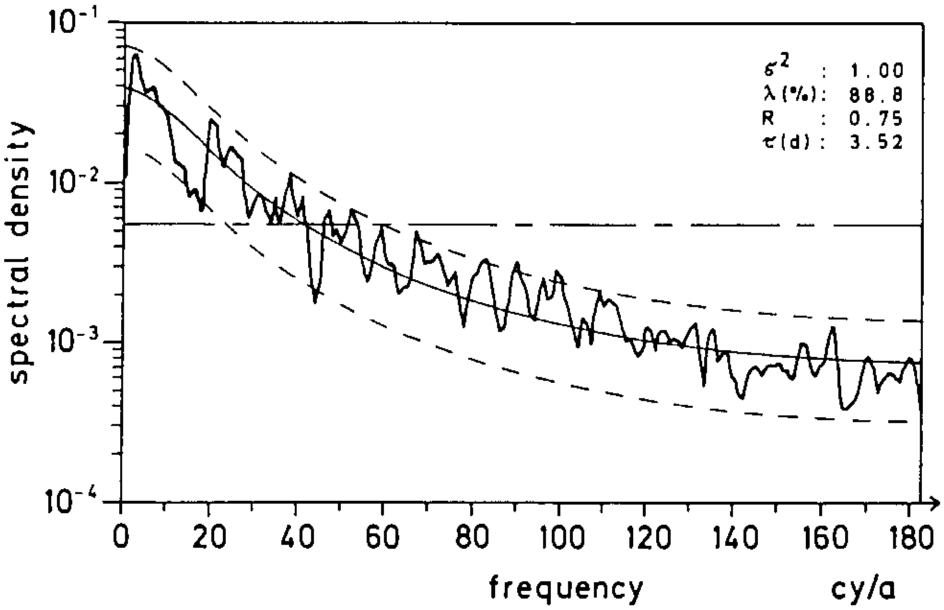

● **Figure 6**
Sample spectrum of the noon temperature amplitude a_1 (thick line) and theoretical red noise spectrum (with R = 0.75, τ_1 = 3.5 d; thin line) with 2.5 % and 97.5% significance levels (dashed). The horizontal line indicates the white noise spectrum with the same overall variance ($\sigma^2 = 1.00$)

Having studied the global and spatial charcteristics of variances, we concentrate now on the temporal structures apparent in the EOFs' normalized amplitudes (compare Equation (6)). Figure 6 shows the sample spectrum of the noon temperature's amplitude a_1. The largest proportion of variance (6.3 %) is contained in the frequency band 3.0 ± 0.5 a^{-1} (equivalent periods: 105 d < T < 146 d). Lower frequencies are represented more weekly (the interannual fluctuations have been removed; see Section 3), and towards higher frequencies the variance density decreases as well. The choice of axes in Figure 6 shows clearly the decrease of variance over two orders of magnitude, but the area below the curve is not proportional to variance. The parameter σ^2 stands for the total variance summed over all frequency bands; the deviation from the theoretical value of unity is less than 0.5 %. A comparison with the theoretical Markov spectrum (R = 0.75; see Equation (9)) and the corresponding 95 % confidence

■ **Table 7** Timescales τ of EOF amplitudes 1 to 4 for different elements and types of analyses (C: data from climate stations, S: data from synoptic stations, compare Tables 4 and 6; unit: days; *italics denote that corresponding EOF is non-significant*).

Anal.	Press		Temperature				Humidity				Cloud Cover				Sunsh.		Rain	
	C	S	C			S	C			S	C			S	C	S	C	S
type	M	M	07	14	21	M	07	14	21	M	07	14	21	M	Σ	Σ	Σ	Σ
τ_1	2.5	2.6	3.6	3.5	3.8	3.9	1.7	1.7	2.0	1.8	1.3	1.2	1.2	1.4	1.3	1.4	0.8	0.9
τ_2	*1.9*	*2.5*	1.4	1.6	1.5	*2.4*	1.5	1.2	1.4	1.8	0.9	0.6	0.8	0.9	0.8	0.7	0.4	0.5
τ_3	*0.9*	*1.4*	*1.1*	*1.4*	*0.9*	*1.4*	1.2	1.2	1.1	*1.2*	0.6	0.7	0.5	*0.8*	0.8	*0.9*	0.5	*0.6*
τ_4	*0.6*	*0.7*	*1.1*	*0.8*	*1.3*	*1.4*	0.8	0.6	0.8	*1.0*	0.4	0.5	0.5	*0.6*	*0.6*	*0.5*	0.4	*0.5*

interval shows that the sample spectrum is not significantly different from the chosen theoretical spectrum. Thus, the amplitudes of EOF1 of the noon temperature do not exhibit significant periodicities, but only persistence with a characteristic timescale $\tau_1 = 3.5$ d.

The amplitude spectra of all analysed elements do not significantly differ (risk level 5%) from the red spectrum of a Markov process. Thus, the characteristik timescale τ as the only relevant measure. Table 7 summarizes these times scales of the amplitudes of the first four EOFs for all analyses discussed above. EOF1 exhibits the most pronounced mean persistence for all elements, which is best developped for temperature ($\tau_1 > 3$ d) and which is more or less non-existent for precipitation ($\tau_1 < 1$ d with a sampling interval of $\Delta t = 1$ d). For all elements, τ decreases with increasing EOF-order; distinct differences related to the time of day or between climate data and synoptic data analyses are not found.

In Summary, we conclude that all the EOF amplitudes exhibit a mean persistence of a few days at the most, as the annual fluctuation had been removed; this appears to be typical for a region within the westerlies with quickly changing weather situations. Nevertheless, it should be noted that the characteristic timescale (as defined in Section 2) is a measure for the *mean* temporal structure of the complete time series. There are singular periods with constantly non-zero amplitude values, e.g. the mild beginnung of spring from 20/3 to 12/4/1974 with frequent Föhn situations (see GEB, 1974) or the hot spell from 19/6 to 9/7/1976. These events are found exclusively in the amplitude of EOF1 as synoptic scale influences lead to parallel deviations from the annual fluctuation for the entire region of analysis (for more details see VOLKERT 1983, pp. 86–89).

So far different meteorological elements were analysed separately. Although the patterns of the principal EOFs are quite similar for e.g. temperature (T), humidity (H) and cloud cover (C; compare Table 4), we have no information about the synchronous enhancement of these EOFs. A compound analysis where the covariance matrix is built from suitably weigthed data of several elements yields this information. It is assumed that all elements are equally important: humidity and cloud cover values are weighted in such a way that Spur $(\mathbf{C}_{TT})$ = Spur $(\mathbf{C}_{HH})$ = Spur $(\mathbf{C}_{CC})$, where indexed **C** stands for the particular element's submatrix; schematically the compound covariance matrix looks like

$$\mathbf{C} = \begin{pmatrix} C_{TR} & \cdot & \cdot \\ C_{TH} & C_{HH} & \cdot \\ C_{TC} & C_{HC} & C_{CC} \end{pmatrix}$$

Here we document the major results of the compound analysis T/H/C (noon values). For technical details and additional information see VOLKERT (1983, pp. 50–51 and pp. 89–98).

Table 8 compares global measures of the T/H/C compound analysis and its separate counterparts. Due to lower threshold values (p = 153; see Table 1) six significantly non-random EOFs are found which ac-

■Table 8 Global variability measures for compound and separate analyses of temperature (T), relative humidity (H) and cloud cover (C); for the compound analysis the relative contribution of each element is also indicated; all data from 14 hours observations; compare Table 4 for detailed explanation.

Analysis units	T/H/C K^2	T	H (rel. contribution)	C	T K^2	H 1	C 1
AV (= Λ)	10920				3640	1.89	5.69
λ_1/Λ	56.5 %	.40	.34	.26	88.8 %	68.7 %	64.4 %
λ_2/Λ	13.0 %	.53	.07	.40	3.7 %	9.0 %	7.7 %
λ_3/Λ	5.8 %	.11	.56	.33		5.0 %	4.7 %
λ_4/Λ	4.6 %	.14	.51	.35		3.0 %	3.0 %
λ_5/Λ	3.0 %	.18	.47	.35			
λ_6/Λ	1.6 %	.16	.45	.39			
q_{sig}	6				2	4	4
$\Sigma\lambda/\Lambda$	84.5 %				92.5 %	85.7 %	79.8 %

count for 85 % of the analysed variance. For the first two, temperature constitutes the most important subvector and for the last four humidity, whereas the cloud cover portion is closer to the average (.33) in all cases. If one were to use EOF analysis as a means to select the minimum number of predictors for statistical forecasts, the compound analysis (here of order 3) is superior to 3 separate analyses (6 EOFs as opposed to 10; see KUTZBACH, 1967, p. 798).

More important, however, seems to be the fact that now two EOFs are of the constant field type combining the subvectors in different ways. EOF1, which accounts for 56 % of variance, stands for the synchronous combination of warmer / dryer / less cloudly [or colder / wetter / more cloudy] than normal for the particular time of the year. EOF2, on the contrary, characterizes the situation colder / (dryer) / less cloudy [or warmer / (wetter) / more cloudy]. The humidity part is put in brackets as it is nearly irrelevant within EOF2 (see Table 8). Inspection of the corresponding amplitudes reveals that EOF1 is more strongly enhanced (in the positive and negative direction) in spring and summer, while EOF2 is activated especially in winter. This coincides with the typically occurence of weather situations conducive to the combinations described above.

EOF3 and EOF4 both contain north-south contrasts for all elements with the combination warmer / dryer / less cloudy. The gradients within the subvectors are more or less parallel, only the zero-lines have different positions. EOF5 and EOF6 exhibit for all elements both kinds of west-east contrasts which have been found in the separate analyses (see Figure 5). The characteristic timescales amount to a little more than two days for the first three EOFs and to less than one day for the last three.

In order to check that the EOFs obtained so far are stable ones (i.e. they are not sensitive to the chosen test period) analyses of two two year subperiods (1974/75 and 1976/77) are carried out. The resulting global measures are nearly identical (see Table 9). The similarity of the corresponding non-random EOFs slowly decreases with increasing EOF order, but is reasonably high even between the EOF3s of both subperiods. Only the timescales exhibit quantitative differences. However, this is not surprising as the timescales are related over the spectrum to the lagged autocovariance function of the EOF amplitude' time series. For the strongly fluctuating amplitudes, the final value of τ is sensitive to the interval in question. More significant than the particular values is the qualitative agreement between the subperiods that the timescales decrease both with EOF order and within the rank order of the elements. Additional checks with analyses for every single year consolidate these findings.

On the contrary, separate investigations for summer and winter reveal that analyses over entire years result in mean variance structures which differ seasonally (see Table 10). The following definition is used: summer from 18/5 to 14/9, winter from 16/11 to 15/3; thus, each sample contains 4x120 days.

■**Table 9** Global variability measures, characteristic timescales and scalar products for temperature, humidity and cloud cover analyses over two subperiods. *Figures for non-significant EOFs in italics.*

Element	T14		H14		C14	
units	K^2		1		1	
years	74/75	76/77	74/75	76/77	74/75	76/77
AV (= Λ)	1230	1260	1.40	1.44	5.39	5.36
λ_1/λ	89.3 %	88.3 %	69.1 %	68.4 %	65.3 %	63.6 %
λ_2/D	3.6 %	4.0 %	9.2 %	9.1 %	7.8 %	7.7 %
λ_3/Λ	*2.1 %*	*2.4 %*	4.8 %	5.4 %	4.3 %	5.2 %
q_{sig}	2	2	3	3	3	3
$\Sigma\lambda/\Lambda$	92.8 %	92.4 %	83.0 %	82.9 %	77.4 %	76.5 %
τ_1 (d)	4.5	2.9	2.2	1.4	1.5	1.0
τ_2 (d)	1.6	1.7	1.2	1.4	0.6	0.6
τ_3 (d)	1.3	1.5	1.1	1.3	0.4	1.0
EOF1·EOF1	1.00		1.00		1.00	
EOF2·EOF2	0.90		0.97		0.96	
EOF3·EOF3	0.89		0.90		0.88	

■**Table 10** Global variability measures for seasonal analyses of temperature, humidity and cloud cover and scalar product between season and corresponding all year EOFs. *Figures for non-significant EOFs in italics.*

Element	T14		H14		C14	
units	K^2		1		1	
season	summer	winter	summer	winter	summer	winter
AV (= Λ)	1250	980	1.54	1.13	5.15	5.78
λ_1/Λ	91.7 %	82.9 %	76.8 %	54.1 %	71.4 %	59.1 %
λ_3/Λ	*2.5 %*	7.2 %	6.7 %	13.7 %	6.1 %	9.5 %
λ_3/Λ	*1.6 %*	*2.8 %*	3.5 %	8.4 %	3.3 %	5.8 %
qsig	1	2	3	4	3	4
$\Sigma\lambda/\Lambda$	91.7 %	90.1 %	87.0 %	80.1 %	80.8 %	78.2 %
EOF1·EOF1	1.00	1.00	1.00	0.99	1.00	1.00
EOF2·EOF2	0.80	0.95	0.90	0.96	0.93	0.97
EOF3·EOF3	0.65	0.93	0.80	0.94	0.70	0.95
EOF4·EOF4	0.73	0.90	0.76	0.91	0.84	0.95

In winter the noon variability of temperature and humidity is reduced by about 20 % relative to summer time observations as the deviations from the annual fluctuation are larger during the summer (equal occurence of positive and negative deviations). On the other hand, cloud cover exhibits 10 % less variance during the summer than during the winter. Furthermore, EOF1 (as usual of the constant field type) is more important for summer days. This may be explained in terms of the higher winter occurence of front passages which are conducive to mesoscale differences in the temperature, humidity and cloud fields (see HOINKA, 1985), and with the greater climatic contrast between Alpine foothills and foreland in winter.

Figure 7 shows EOF2 of temperature for both seasonal samples. The summer field is characterized by a steady gradient between the contrasting regions Allgäu and Bayrischer Wald. In winter we find a narrow band of isolines along the Alpine foothills and the Bayrischer Wald, which indicates that temperature gradients are mostly confined to these small regions. On the whole, all non-random winter EOFs are more similar to the all year EOFs (scalar product > 0.90; see Table 10) than is the case for the typical summer structures.

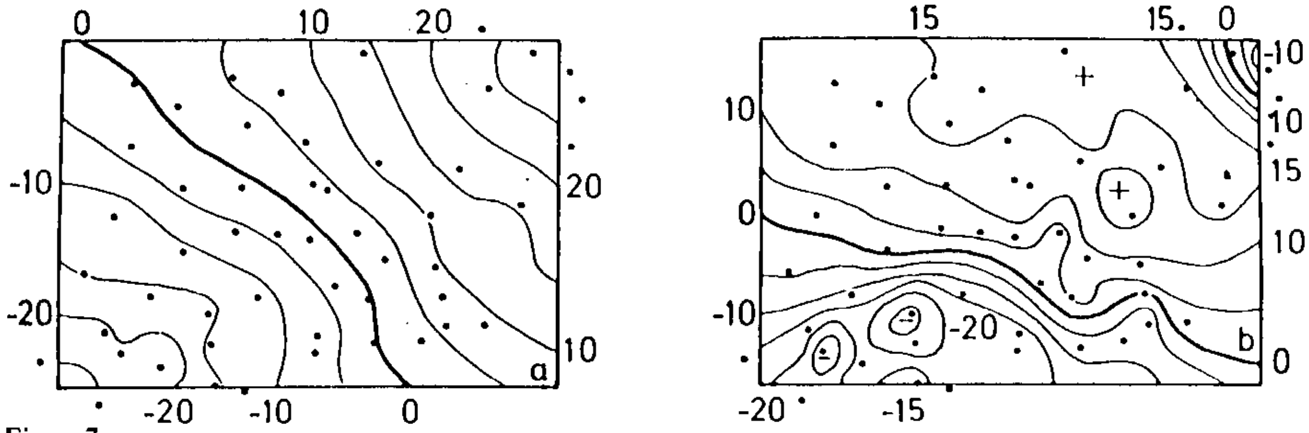

Figure 7

Seasonal EOF2 for noon temperature; calculated from summer days (18/5 to 14/9; a) and winter days (16/11 to 15/3; b) of the period 1974 through 1977. Labels in hundredths of dimensionless units.

5 Conclusions

In the presented study we have applied the techniques of empirical orthogonal functions and frequency analyses with corresponding statistical tests to data collected on a routine basis at second order climatological stations. Various quantitative information were obtained about the spatial and temporal variability of the meteorological elements investigated (pressure, temperature, relative humidity, cloud cover, daily sunshine duration and daily precipitation).

All analyses exhibit a constant field over the whole of Southern Bavaria as major variability structure. Its relative importance determines a rank order within the analysed elements. A common north-south contrast is found as the most important mesoscale structure that modulates the constant field type deviation. This is related to the position of Southern Bavaria relative to the Alpine barrier, which determines the spatial structures of many weather situations (e.g. Föhn events, precipitation on the windward side of the Alps, winterly high pressure blocking situations with persistent stratus above the foreland). Only the following EOF modes contain west-east contrasts as one expects for a region within the belt of prevailing westerlies.

Furthermore, a compound analysis for temperature, humidity and cloud cover reveals how positive and negative deviations of the different elements are synchronously combined. The first two EOFs are different combinations of the constant field type which can be identified as model weather situations, which typically occur in different seasons. Characteristic timescales lie in the order of a few days at most, and decrease both with EOF order and with the position in the rank order of elements. Indeed, they agree with the mean duration of low or high pressure situations in Central Europe. No significant periodicities are encountered. The variability structures found appear to be stable for entire years, whereas separate seasonal analyses show distinct differences between winter and summer. Further investigations with subsamples (Föhn events and abundant areal precipitation; not reported here, but documented in VOLKERT, 1983, pp. 112–134) suggest that the results presented are typically for Southern Bavaria.

The detailed analysis of variance appears to be an adequate and easy tool for studies concerning the variability of meteorological fields about their mean values. There are no immediate restrictions which would prevent applications with larger networks and longer time series. The computing time depends linearly on the length of the time series and at most in a quadratic way on the number of stations.
As long as one uses standard diagonalisation methods which keep the full matrix in core, the memory requirement depends quadratically on the number of stations.

In order to better demonstrate the dependence of the analysed north-south contrast on the Alps, future applications should incorporate stations in Switzerland, Baden-Württemberg and Austria. A ten year period would offer better possibilities for stability studies. The main difficulty for such a project is seen in the acquisition of a suitable, computerized dataset. The availability of numerical mesoscale models on a quasioperational basis would strongly motivate such applications as a means for the verification of longer series of model output. Additionally, an expansion into empirical orthogonal functions could be used as standard data compression tool for datasets collected at high sampling rates with an automatically operating network (e.g. the Swiss ANETZ; see JOSS, 1980).

Acknowledgement

The analysed datasets, which constitute the basis of this study, were provided by the Deutscher Wetterdienst (DWD). The data transfer was organized by the Klimaabteilung of the Zentralamt in Offenbach; further information was made available through the Wetteramt München and the Observatorium Hohenpeißenberg. I would like to thank all the staff of these institutions, who had to deal with me, for their assistance. Furthermore, I am indebted to J. EGGER for his advice and supervision during the dissertation project that led to the research presented here. The help by G. KÖRNER is acknowledged for preparing most of the figures.

References

ATTMANNSPACHER, W. (Ed.), 1981: 200 Jahre meteorologische Beobachtungen auf dem Hohenpeißenberg. Ber. Deut. Wetterdienst Nr. 155, 84 pp.

CAPPEL, A., 1980: Societas Meteorologica Palatina (1780–1795). Ann. Meteorol. (N.F.) Nr. 16, 10–27.

CAPPEL, A. und M. KALB, 1976: Das Klima von Hamburg. Analyse für Zwecke der angewandeten Klimatologie mit Datenkatalog. Ber. Deut. Wetterdienst Nr. 141, 247 pp.

CEHAK, K., 1983: Alpenklimatologie – Ein Statusbericht. Wetter und Leben 34, 227–240.

DAVIS, R., 1976: Predictability of Sea Surface Temperature and Sea Level Pressure Anomalies over the North Pacific Ocean. J. Phys. Oceanogr. 6, 249–266.

FLIRI, F., 1967: Beiträge zur Kenntnis der Zeit-Raum-Struktur des Niederschlags in den Alpen. Wetter und Leben 19, 241–268.

FRAEDRICH, K. and K. MÜLLER, 1983: On Single Station Forecasting: Sunshine and Rainfall Markov Chains. Beitr. Phys. Atmosph. 56, 108–134.

GEB, M., 1974: Klimatologische Übersicht für März 1974. Beilage zur Berliner Wetterkarte vom 23.4.1974, Meteorol. Inst. FU Berlin, 4 pp.

HOINKA, K., 1985: On Fronts in Central Europe. Beitr. Phys. Atmosph. 58.

HÜSTER, H., 1980: Darstellung der täglichen Bodendruckfelder (1881–1975) im europäisch-ostatlantischem Sektor durch empirische Orthogonalfunktionen. Dissertation, Universität Bonn, 92 pp.

JENKINS, G. and D. WATTS, 1968: Spectral Analysis and its Applications. San Francisco: Holden Day, 525 pp.

JOSS, J., 1980: Projekt ANETZ: Konzept und Realisierung eines Netzes von automatischen Wetterstationen in der Schweiz. Ann. Meteorol. (N.F.) Nr. 16, 33–35.

KUTZBACH, J. 1967: Empirical Eigencectors of Sea-Level Pressure, Surface Temperature and Precipitation Complexes over North America. J. Appl. Meteor. 6, 791–802.

LORENZ, E., 1959: Prospects for Statistical Weather Forecasting. Mass. Inst. Tech. Report, Cambridge (Mass.), 185 pp. (available from Zentralbibliothek des DWD, D-6050 Offenfach)

MASON, B. J., 1979: Some Results of Climate Experiments with Numerical Models. WMO Publication Nr. 537, Geneva, 210–242.

MITCHELL, J. (Ed.), 1966: Climatic Change. WMO Technical Note No. 79, Geneva, 79 pp.

ORLANSKI, I., 1975: A Rational Subdivision of Scales for Atmospheric Processes. Bull. Amer. Meteor. Soc. 56, 527–530.

OVERLAND, J. and R. PREISENDORFER, 1982: A Significance Test for Principal Components Applied to a Cyclone Climatology. Mon. Wea. Rev. 110, 1–4.

PREISENDORFER, R., F. ZWIERS and T. BARNETT, 1981: Foundations of Principal Component Selection Rules. SIO Reference Series 81-4, Scripps Institution of Oceanography, La Jolla, California, 192 pp.

SCHÄFER, P., 1982: Das Klima ausgewählter Orte der Bundesrepublik Deutschland – München. Ber. Deut. Wetterdienst Nr. 159, 256 pp.

SCHIRMER, H., 1969: Langjährige Monats- und Jahresmittel der Lufttemperatur und des Niederschlags in der Bundesrepublik Deutschland für die Periode 1931–1960. Ber. Deut. Wetterdienst Nr. 115, 28 maps + 32 pp.

SCHIRMER, H. and V. VENT-SCHMIDT, 1979: Das Klima der Bundesrepublik Deutschland – Lieferung 1: Mittlere Niederschlagshöhen für Monate und Jahre, Zeitraum 1931–1960. Deutscher Wetterdienst, Offenbach, 16 maps + 69 pp.

SCHÖNWIESE, C. 1974: Schwankungsklimatologie im Frequenz- und Zeitbereich. Wiss. Mitt. Meteorol. Inst. Univ. München Nr. 24, 137 pp.

SCHÖNWIESE, C., 1979a: Klimaschwankungen. Berlin, Springer, XII + 181 pp.

SCHÖNWIESE, C., 1979b: Correlations and Phases of Band-pass Filtered European Air Temperature Series. Beitr. Phys. Atmosph. 52, 136–146.

VOLKERT, H., 1983: Klimatologie der Varianz meteorologischer Felder in Südbayern. Dissertation, Universität München, 154 pp. (also available as Research Report DFVLR-FB 83–31)